Materials Physics and Mechanics 13 (2012) 175-180 Received: March 13, 2012

ZINC OXIDE TETRAPOD SYNTHESIS AND APPLICATION FOR UV SENSORS

S. Rackauskas*, T. Talka, E.I. Kauppinen, A.G. Nasibulin

NanoMaterials Group, Department of Applied Physics, Aalto University

Puumiehenkuja 2, 00076, Espoo, Finland

*e-mail: simas.rackauskas@aalto.fi

Abstract: Zinc oxide tetrapods (ZnO-Ts) were synthesized by air oxidation of zinc vapor. For stable production of the ZnO-Ts at the furnace temperatures of 900 °C, the lowest evaporator temperature was found to be 480 °C. Aerosol measurements showed that the fraction of naturally charged particles decreased with evaporator temperature from 89 % at 480 °C to 43 % at 420 °C. Various UV sensors were prepared to study the response and reset times and the On/Off ratio as a function of the ZnO-T concentrations, interelectrode distance and air humidity conditions. The presence of humid air was found to increase the conductivity of the ZnO-T sensors and to lower the response and reset times as well as On/Off ratio to 98, 96 and 88 %, respectively.

1. Introduction

Zinc oxide is an n-type semiconductor compound belonging to the group of II-IV semiconductor materials. Due to its direct wide band-gap of 3.37 eV and an exciton binding energy of 62 meV, it is one of the most promising semiconductor materials for fabricating optoelectronic devices that operate in blue and ultraviolet (UV) region [1, 2]. Non-catalytically grown ZnO nanostructures can be observed in various morphologies such as nanowires [3], nanobelts [4], nanobridges and nanonails [5], nanoshells [6], tetrapods [7]. Significant properties of ZnO are its radiation hardness and a capability for band-gap tuning by alloying with metals such as magnesium or cadmium [8]. In addition to optoelectronic features of ZnO, there are several other characteristics that have gained remarkable attention, including: pyroelectricity [9], piezoelectricity and transparent conductivity [8]. The ZnO nanocrystal size and shape attributed properties are crucial when designing wide range of applications such as gas sensors [10], field effect transistors (FETs) [11], flame sensors, UV sensors and missile plume detectors [8]. ZnO nanostructure synthesis is carried out by either vapor-solid (VS) or vapor-liquid-solid (VLS) growth mechanism.

ZnO tetrapods (ZnO-Ts) were synthesized in a vertical flow reactor described in our previous publication [7]. In this work we carried out more detailed investigations of ZnO-T formation. We aimed to stabilize the tetrapod synthesis by lowering an evaporation temperature. Aerosol measurements were carried out to study charging of ZnO-Ts in the gas phase. And finally to optimize the performance of ZnO-T UV sensors, we investigated the effect of the tetrapod concentration, electrode distances, and air humidity on On/Off ratio, response and reset times.

2. Experimental methods

Synthesis of ZnO-Ts was described elsewhere [12]. Briefly, ZnO-Ts were synthesized by a gas phase oxidation of Zn vapor in an air atmosphere. The synthesis reactor consisted of a

vertical quartz tube inserted in a furnace, a metal evaporator inside the tube and the product collection system. The metal evaporator was a stainless steel tube filled with Zn powder (99.999 % purity). Argon (99.999 %), purified from oxygen containing species by an oxygen trap (Agilent OT3-4), was utilized as a carrier gas through the evaporator at the flow rate of 0.3 L/min. An outer air flow was introduced in the reactor at the flow rate of 1.0 L/min. An average residence time in the reactor was varied from 1.9 to 2.6 s. Produced ZnO-Ts were collected downstream of the reactor on a nitrocellulose filter or supplied to differential mobility analyzer (DMA) for aerosol measurements.

To investigate the charging phenomenon, the flow from the reactor with ZnO-Ts was introduced via an electrostatic filter (ESF) to a DMA and a Condensation Particle Counter (CPC) to measure the mobility diameter distribution of the product. To estimate the fraction of charged aerosol particles, the first scan was performed with no voltage applied to the ESF and the following two scans were carried out right after each other at 6.3 kV. The concentration obtained with applied voltage was averaged. In the measurements TSI Model 3071 DMA with TSI Model 3775 CPC and Grimm Vienna/Reischl Type DMA, Grimm Model 5.710 DMA Controller with Grimm Model 5414 CPC were used. The product was investigated by a scanning electron microscope (SEM, JEOL JSM 7500F).

For ZnO-T based UV sensors Pd/Au electrodes with interelectrode gap distances of 2, 5, and 13.5 mm were deposited on polyethylene terephthalate (PET) substrates by sputtering. ZnO-Ts were deposited on the electrodes from a ZnO-T/MEK (Methyl Ethyl Ketone) solution. Two ZnO-T concentrations of 1 mg/cm^2 and 2 mg/cm^2 were examined.

In the experiments the UV sensors were placed inside a quartz tube. Both dry and humid air were introduced at the flow rates of 1000 cm^3/min. Humid flow was introduced by bubbling air through water at room temperature. A UV source was placed 5 cm above the tube and the sensors were illuminated with an intensity of 30 μW/cm^2 at the wavelength of 365 nm. During the experiments the temperature in the laboratory was kept at 20 °C and relative humidity at 62 %. Sensors with different electrode distances were studied by turning the UV source on and off with 60 second intervals. Response time was calculated from the initial value of the voltage to 90 % of its maximum value, while the reset time was the time to decay to 1/ *e* of its initial value. UV sensor response was measured with a digital oscilloscope (Tektronix DPO 2014) by a comparison method, where the magnitudes of the reference resistor and the UV sensor were compared by the voltage drop they inflicted to the circuit (Fig. 1). A constant potential (20 V) was applied over UV sensor and the reference resistor (0.500 TΩ) connected in series. The voltage drop over the reference resistor was recorded in time while UV illumination was turned on and off. Current flowing through the circuit was later resolved by applying Kirchhoff's law.

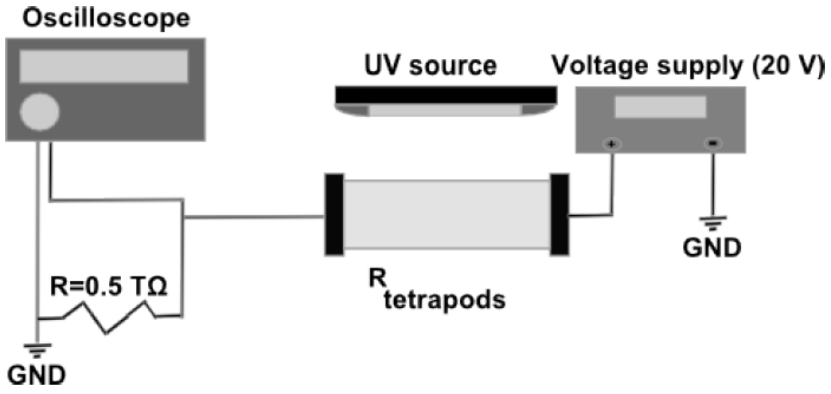

Fig. 1. Schematics of the UV response measuring circuit.

3. Results and discussion

To stabilize the process of the tetrapod synthesis, we attempted to lower the evaporation temperature. The furnace temperature was set to 900 °C and the evaporator temperature was varied from 420 to 550 °C. The evaporator temperature had a great impact on the morphology of the products. It was found that ZnO-Ts with high aspect ratio legs (with the length of 300 nm or longer) and a diameter of 20-100 nm can be obtained at the evaporator temperature above 480 °C (Fig. 2). At lower temperatures only nearly spherical particles and some tetrapods with low aspect ratio legs can be synthesized.

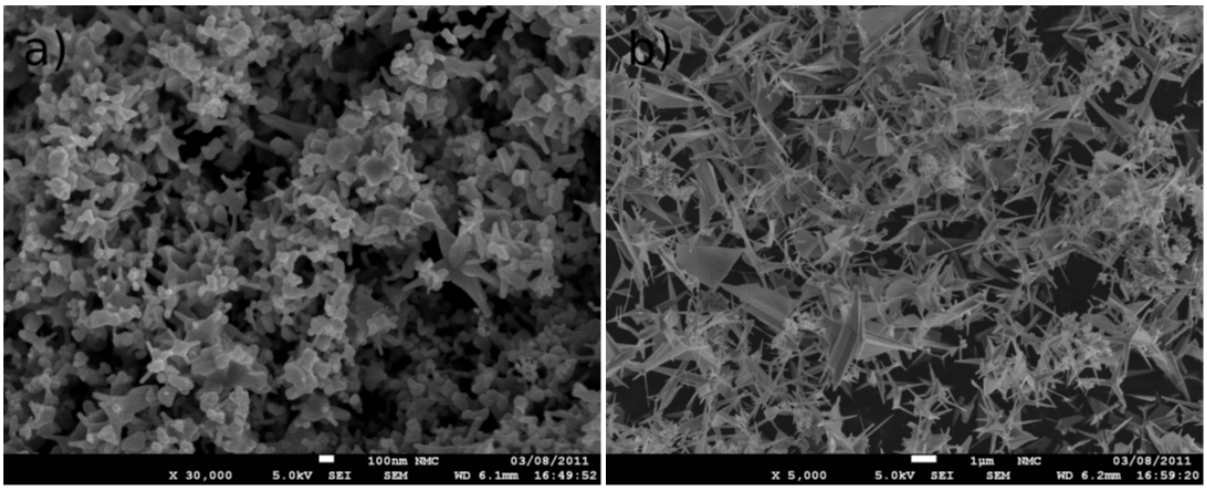

Fig. 2. Zinc oxide particles produced at the furnace temperature of 900 °C and at the evaporator temperature of a) 420 °C; b) 480 °C.

DMA measurements were also carried out at the furnace temperature of 900 °C. Fig. 3 shows the mobility diameter distributions with and without the ESF at the evaporator temperatures of 420, 450, and 480 °C. As can be seen, the mobility distribution peak shifts from 220 nm to about 100 nm as the evaporator temperature decreases from 480 to 420 °C. Similar trend was found for the total concentration of the aerosol particles, which can be explained by the decrease in the concentration of zinc vapor at lower evaporation temperature.

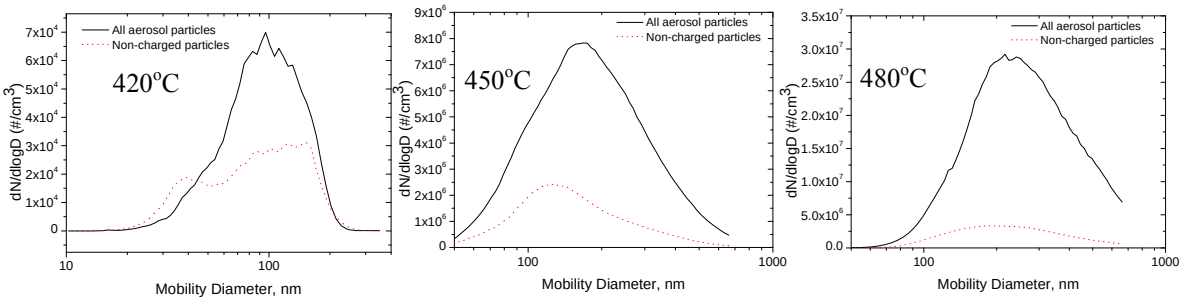

Fig. 3. Number size distribution of the tetrapods synthesized at furnace temperature 900 °C and different evaporator temperatures.

From the graphs one can also estimate the fraction of non-charged aerosol particles. At the evaporator temperature of 480 °C the fraction of non-charged particles is 11 %, at 450 °C the fraction is 23 % and at 420 °C it is 57 %. This observation shows that the concentration of naturally charged particles increases as the temperature increases. This spontaneous charging phenomenon has been reported earlier for iron oxide particles and carbon nanotubes [13],

where a similar temperature dependence on the charged particle concentration was explained by aggregation processes. The latter result in the energy release is due to the minimization of the surface energy and emission of electrons and positive adsorbent molecules.

The UV responses in dry and humid air for sensors prepared from 1 and 2 mg/cm^2 are shown in Fig. 4 and Fig. 5. The 2 mg/cm^2 sensor with the 13.5 mm gap did not give any response to UV light. The 2 mg/cm^2 sensor at the conditions of humid air shows significantly lower response and reset times as can be seen in Fig. 4 b. For the gaps of 2.0 mm and 5.0 mm the response time in humid air decreased by 98 % and 96 %, respectively. Similarly, for any gap size and any ZnO-T concentration, response and reset were always quicker in case of the humid air. At the same time, the humid air decreases the On/Off ratio, which can be seen in Figs. 4a, 5a and 5b. The effect of humidity on the UV sensor characteristics can be attributed to the change in adsorption and desorption rate of oxygen species in dry and humid air.

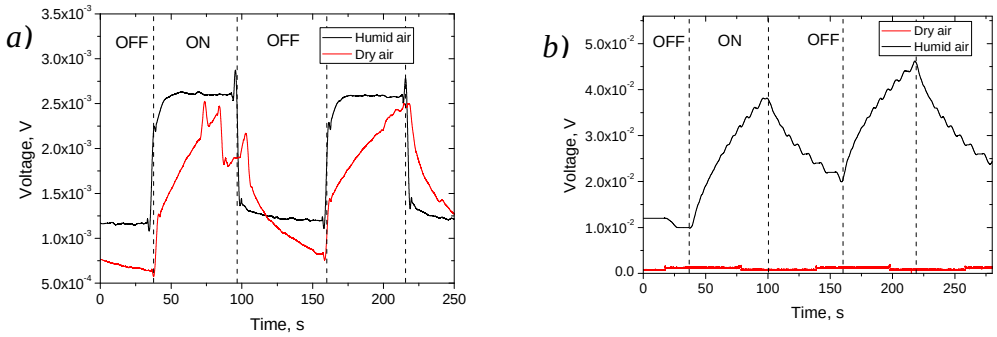

Fig. 4. UV response of the 2 mg/cm^2 sensor under conditions of dry and humid air with different electrode distances: a) 2.0 mm; b) 5.0 mm.

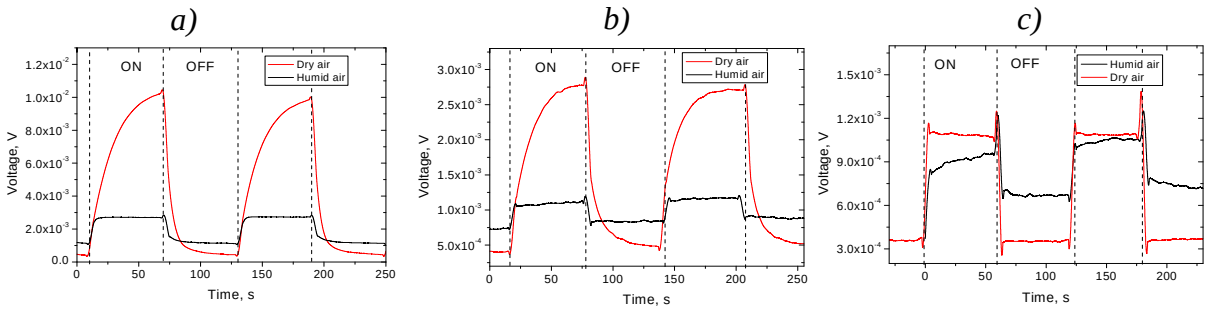

Fig. 5. UV response of the 1 mg/cm^2 sensor under conditions of dry and humid air with different electrode distances: a) 2.0 mm b) 5.0 mm c) 13.5 mm.

The response and reset times and On/Off ratios for each electrode distances are presented in Table 1. As the reset and response times show no clear dependence on the electrode distance, the On/Off ratio clearly decreases with the gap increase. This can be explained by the need for more adsorption (and desorption) of oxygen species to form (to break) the percolation path between electrodes.

In order to exclude the humidity effect on the sensor, the same sensors were examined without UV illumination. The voltage of a 1 mg/cm^2 sensor with the electrode distance of 2.0 mm was measured first under dry air conditions and then in the presence of humid air. The results are shown in Fig. 6 and reveal practically no humidity effect on the device. The only difference was observed in the device noise decrease in the humid air and a very slight voltage increase after 30 s.

Table 1. UV response of the 1 mg/cm^2 and 2 mg/cm^2 sensors under conditions of dry and humid air with different electrode distances. (n.r. - no response).

	Electrode gap, mm						
	2.0		5.0		13.5		
	Dry	Humid	Dry	Humid	Dry	Humid	
Response time, s	32.9	3.7	27.3	1.5	0.9	1.2	1 mg/cm^2
Reset time, s	5.6	1.8	8.2	0.2	3.6	1.7	
ON/OFF ratio	19.7	2.4	5.2	1.3	2.9	1.6	
Response time, s	43.2	6.2	55.0	1.2	n.r.	n.r.	2 mg/cm^2
Reset time, s	24.1	1.5	36.2	1.4	n.r.	n.r.	
ON/OFF ratio	3.0	2.1	2.3	1.6	n.r.	n.r.	

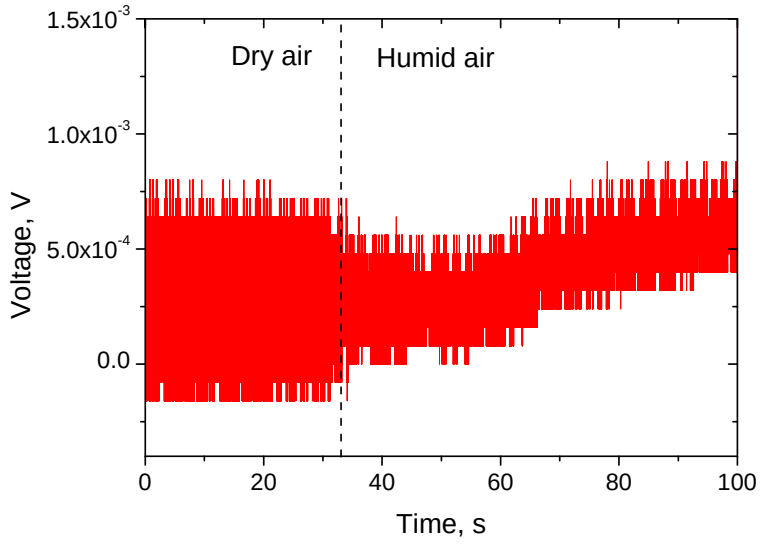

Fig. 6. Effect of humid air on conductivity in the ZnO-T sensor without UV illumination.

4. Conclusions

In summary, ZnO-Ts with various morphologies and sizes were synthesized during zinc vapor oxidation by air at 900 °C. For stable ZnO-T production, the lowest evaporator temperature was found to be 480 °C. The DMA measurements showed that the concentration of naturally charged particles decreased from 89 % to 43 % as the evaporator temperature respectively decreased from 480 to 420 °C. This phenomenon was explained by aggregation processes aiming to minimize the surface energy of tetrapods and energy release leading to the emission of electrons and impurities from the ZnO-Ts. The measurements also revealed that the mean diameter and ZnO-T aerosol concentration decreased with the decrease of the evaporator temperature.

The measurements of the UV sensors prepared from ZnO-Ts showed that the presence of humid air decreased both response and reset times to 98 and 96 %, respectively. Humid air also decreased the On/Off ratio to 88 %. The effect of the humidity on the UV sensor performance can be explained by the need for more adsorption (and desorption) of oxygen species to form (to break) the percolation path between electrodes. The effect of humid air examined without the UV illumination, is found no sensing ZnO-T effect of the water vapor.

The authors thank Dr. Olga Klimova for previous studies on ZnO-T synthesis. The authors are grateful to Kimmo Mustonen for his help with installation of the UV sensor setup. This work was supported by Academy of Finland.

References

[1] Gao-Ren Li, Wen-Xia Zhao, Qiong Bu, Ye-Xiang Tong // *Electrochemistry Communications* **11** (2009) 282.
[2] Z.L. Wang, J.H. Song // *Science* **312** (2006) 242.
[3] Simas Rackauskas, Albert G. Nasibulin, Hua Jiang, Ying Tian, Gintare Statkute, Sergey D. Shandakov, Harri Lipsanen, Esko I. Kauppinen/ *Applied Physics Letters* **95** (2009) 183114-3.
[4] Z.W. Pan, Z.R. Dai, Z.L. Wang *// Science* **291** (2001) 1947.
[5] J. Y. Lao, J. Y. Huang, D. Z. Wang, Z. F. Ren// *Nano Letters* **3** (2003) 235.
[6] Y.H. Leung, K.H. Tam, A.B. Djurišić, M.H. Xie, W.K. Chan, Ding Lu, W.K. Ge // *Journal of Crystal Growth* **283** (2005) 134.
[7] Yong Ding, Zhong Lin Wang, Tianjun Sun, Jieshan Qiu // *Applied Physics Letters* **90** (2007) 153510-3.
[8] S.S. Hullavarad, N.V. Hullavarad, P.C. Karulkar, A. Luykx, P. Valdivia// *Nanoscale Research Letters* **2** (2007) 161.
[9] C.-C. Hsiao, K.-Y. Huang, Y.-C. Hu // *Sensors* **8** (2008) 185.
[10] M.C. Newton, P.A. Warburton // *Materials Today* **10** (2007) 50.
[11] Donald J. Sirbuly, Matt Law, Haoquan Yan, Peidong Yang// *Journal of Physical Chemistry B* **109** (2005) 15190.
[12] S. Rackauskas, K.M.T. Jarvinen, M. Mattila, O. Klimova, H. Jiang, O. Tolochko, H. Lipsanen, E. Kauppinen, A. Nasibulin // *Nanotechnology* **23** (2012) 095502.
[13] Albert G. Nasibulin, Sergey D. Shandakov, Anton S. Anisimov, David Gonzalez, Hua Jiang, Marko Pudas, Paula Queipo, Esko I. Kauppinen // *Journal of Physical Chemistry C* **112** (2008) 5762.